JOURNAL OF AGRICULTURAL AND FOOD CHEMISTRY

Article

pubs.acs.org/JAFC

Thermodynamics of Antimicrobial Peptide JCpep8 Binding to Living *Staphylococcus aureus* as a Pseudo-stationary Phase in Capillary Electrochromatography and Consequences for Antimicrobial Activity

Jianhui Xiao, Hui Zhang,* and Shaodong Ding

State Key Laboratory of Food Science and Technology and School of Food Science and Technology, Jiangnan University, 1800 Lihu Avenue, Wuxi 214122, People's Republic of China

ABSTRACT: To understand the details of the permeation pathways of antimicrobial peptide JCpep8, the antimicrobial processes were investigated step by step in this paper. First, the characterization of the initial binding process was explored by introducing the living *Staphylococcus aureus* cells (LSACs) into electrophoretic buffer used as pseudo-stationary phase in capillary electrochromatography (CEC), and the thermodynamic parameters were determined. The binding constants at 298, 303, and 309 K were 7.40×10^{11}, 1.43×10^{12}, and 2.6×10^{12} M^{-1}, respectively, which indicated the evident interaction between JCpep8 and LSACs. This binding process was spontaneous. Both the electrostatic force and hydrophobic effect play major roles in this binding process. Second, antibacterial activity kinetics and outer membrane and inner membrane disruption assays were investigated. Data indicated that JCpep8 killed microbes principally by breaking their cell wall and membrane, followed by cell lysis. The results were confirmed by Fourier transform infrared (FTIR) spectroscopy and transmission electron microscopy (TEM). In summary, JCpep8 kills microbes mainly by wall-/membrane-targeting pore-forming mechanisms.

KEYWORDS: *Antimicrobial peptide, antimicrobial detail, capillary electrochromatography (CEC), living Staphylococcus aureus cells*

INTRODUCTION

With the extensive use of antimicrobial drugs for a long time, drug-resistant strains have been increasing and becoming a serious problem, affecting public health all over the world. To overcome this problem, researchers have begun to look for a new generation of antibacterial agents. Antimicrobial peptides (AMPs) with anticancer activities and broad-spectrum antimicrobial activities, which do not induce the generation of drug-resistant strains, may be a promising candidate.[1−4]

Recently, four antibacterial models[5−12] (barrel-stave, toroidal pore, sinking-raft, and carpet models), which were explored by studying the interaction of AMPs with model membranes composed of synthetic lipids, have been proposed for the mechanisms of AMPs.

However, AMPs act in a complex environment, such as the living cell. Additionally, the varied AMPs may have significant differences in the mode of antimicrobial action and mechanisms. For those reasons, the four proposed models might be too rigid to cover all of the mechanisms of AMPs. However, no matter what kind of antibacterial modes and environment, AMPs must initially bind to the living bacterial cells.[1,13] More importantly, the initial interaction processes with the living bacterial cells significantly influence the antimicrobial dynamics and membrane-disrupting effects of subsequent AMPs.[1,13] Consequently, characterizing the initial interaction processes of AMPs in the living cell environment may be helpful for the design of membrane-selective therapeutic agents and the evaluation of their pharmaceutical activity and chemical toxicity.[1,13−15] Nevertheless, there have been few reports on the details of the permeation pathways of AMPs in the living cell environment up to now.

Therefore, aiming at discovering the details when AMPs bind to the living bacteria, a series of concentrations of the living *Staphylococcus aureus* cell (LSAC) suspensions in the running buffer were used as a pseudo-stationary phase to characterize the binding processes of JCpep8 to LSACs by capillary electrochromatography (CEC) in this paper. At the same time, the binding constant and thermodynamic parameters, such as interaction forces, enthalpy change, entropy change, and free energy change, were determined during the process. Furthermore, the action kinetic and mechanism models of JCpep8 were investigated by time-dependent experimental settings, such as antibacterial activity kinetics and outer and inner membrane disruption assays, as well as the bacterial ultrastructure.

MATERIALS AND METHODS

Materials. JCpep8 [AMPs, CAILTHKR; minimal inhibitory concentration (MIC) for *S. aureus*, 45 μg/mL], screening from *Jatropha curcas* by cell membrane affinity chromatography, was provided by the School of Food Science and Technology, Jiangnan University. *S. aureus* American Type Culture Collection (ATCC) 25923 was provided by the Wuxi Disease Prevention and Control Center (Wuxi, China). Tris, polyethylene oxide (PEO; M_w = 600 000), boric acid, ethylenediaminetetraacetic acid (EDTA), 1,8-anilinonaphthalenesulfonate (ANS), and propidium iodide were purchased from Sigma (St. Louis, MO). All other regents were of analytical grade and purchased from Sinopharm Chemical Reagent Factory Co., Ltd. (China).

Microbe Preparation. *S. aureus* was cultured to the mid-log phase and centrifuged at 5000*g* for 5 min. The precipitate was collected, washed by the running buffer, and then centrifuged again. This

Received: December 21, 2011
Revised: March 28, 2012
Accepted: April 2, 2012
Published: April 2, 2012

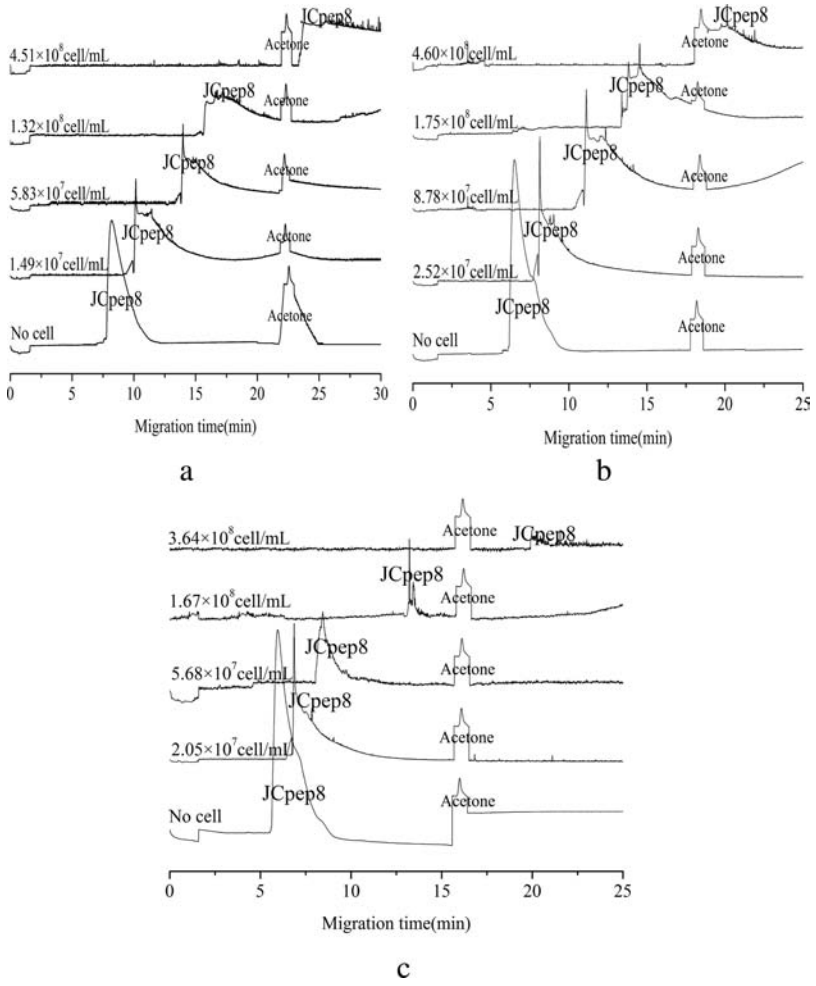

Figure 1. Electropherograms of JCpep8 with the binding completed at (a) 298 K, (b) 303 K, and (c) 309 K. The running buffer contained increasing amounts of LSACs. The conditions used were as follows: Beckman P/ACE MDQ capillary electrophoresis system; injection, 0.8 psi for 8 s; applied voltage, 25 kV; detection, UV detection at 220 nm; and capillary, capillary of 65 cm × 75 μm inner diameter.

washing step was repeated 3 times. The washed precipitate was resuspended in the running buffer with a series of cell concentrations.[16] The mass of LSACs in a 10^7 cell/mL solution was estimated by microbiologists (10^7 cell/mL consists of 58 μg of bacteria).[17] Before each experiment, the LSAC suspension was dispersed by ultrasonics for 1.5 min.

Buffer Preparation. The experiment was performed according to Szumski et al.,[16] with some modifications. The stock buffer solution (pH 7.5) containing 4.5 mM Tris, 4.5 mM boric acid, and 0.1 mM EDTA (TBE buffer) was prepared in deionized water. The 0.25% PEO solution was prepared in that stock buffer solution, then treated by ultrasound for 5 h at 50 °C, and left overnight to dissolve completely. The running buffer solution was prepared by diluting the stock PEO solution with TBE buffer to a final concentration of 0.0125%. All buffers and PEO solutions were freshly prepared daily.

CEC Conditions. All experiments were performed on a Beckman P/ACE MDQ (Beckman Coulter, Pasadena, CA) with a 65 cm × 75 μm inner diameter (57 cm to the detector) uncoated fused-silica capillary (Hengyao Chromatogram Equipment Co., Ltd., Shanghai, China). The new capillary was first rinsed with 1 M NaOH at 60 °C for 10 min and then rinsed with deionized water for 10 min and running buffer at 36 °C for 15 min. Injection was performed at 0.8 psi for 8 s. Between all runs, the capillary was conditioned by aspirating 1 M NaOH, deionized water, 1 M HCl, and running buffer for 5 min at 50 psi pressure. The detector signals were recorded at 220 nm. Positive polarity mode with 25 kV was used throughout the experiments. The capillary temperature was kept at 298, 303, and 309 K.

Binding Constant. The experiment was performed according to Tanaka and Terabe,[18] with some modifications. The concentration of JCpep8 is the MIC (45 μg/mL) for *S. aureus* in these experiments. The binding constant was calculated by the following Scatchard equation:

$$\mu_0 - \mu = -\frac{1}{K[C]}(\mu_0 - \mu) + b \quad (1)$$

$$y = ax + b \quad (2)$$

where μ_0 and μ are the effective mobilities of JCpep8 in the absence and presence of LSACs in the running buffer, respectively, $[C]$ is the concentration of LSACs in the running buffer, y is $\mu_0 - \mu$, x is $1/[C](\mu_0 - \mu)$, a is $-1/K$, and K is the binding constant at the corresponding temperature. Therefore, the binding constant of JCpep8 to LSACs is calculated from eq 2, which is the linear least-squares method based on the experimental data.

Thermodynamic Parameters. The experiment was performed according to Ross and Subramanian,[19] with some modifications. The thermodynamic parameters including enthalpy change (ΔH), entropy change (ΔS), and free energy change (ΔG) can be evaluated using the following equations:

$$\ln K = -\Delta H/RT + \Delta S/R \quad (3)$$

$$\Delta G = \Delta H - T\Delta S \quad (4)$$

where R is the gas constant. On the basis of the K values of JCpep8 with LSACs and the linear relationship of ln K versus $1/T$, ΔH and ΔS

Table 1. Experimental Data for the Interaction between JCpep8 and LSACs at 298, 303, and 309 K

	cell concentration		migration time (min)		electrophoretic mobility ($cm^2\ kV^{-1}\ min^{-1}$)		regression study	
temperatures (K)	cell/mL	mg/mL	acetone	JCpep8	EOF	JCpep8	parameter	value
298	0	0	22.53	8.12	6.58	11.67	slope	-4.7298 kV min cm^{-2} M
	1.49×10^7	0.087	22.24	10.16	6.66	7.92	intercept	60.107 kV min cm^2
	5.83×10^7	0.34	22.16	14.01	6.69	3.89	r^2	0.9923
	1.32×10^8	0.77	22.31	17.13	6.64	2.01		
	4.51×10^8	2.63	22.38	23.76	6.62	-0.38	K_{RL}	$7.40 \times 10^{11}\ M^{-1}$
303	0	0	18.17	6.47	8.16	14.75	slope	-2.4445 kV min cm^{-2} M
	2.52×10^7	0.147	18.23	8.17	8.13	10.01	intercept	43.135 kV min cm^2
	8.78×10^7	0.512	18.34	11.11	8.08	5.26	r^2	0.993
	1.75×10^8	1.02	18.23	14.55	8.13	2.06		
	4.60×10^8	2.68	18.42	20.15	8.05	-0.69	K_{RL}	$1.43 \times 10^{12}\ M^{-1}$
309	0	0	15.99	5.95	9.27	15.64	slope	-1.3473 kV min cm^{-2} M
	2.05×10^7	0.12	16.09	6.86	9.21	12.39	intercept	31.88 kV min cm^2
	5.68×10^7	0.331	16.11	8.49	9.20	8.26	r^2	0.9932
	1.67×10^8	0.972	16.21	13.43	9.14	1.89		
	3.64×10^8	2.12	16.16	19.32	9.17	-1.50	K_{RL}	$2.60 \times 10^{12}\ M^{-1}$

were calculated from the slope and intercept according to eq 3. Then, ΔG was calculated from eq 4.

Growth Inhibition Curve Assay. The experiment was performed by the liquid growth inhibition assay according to Hultmark et al.,[20] with some modifications. *S. aureus* of mid-log phase was centrifuged at 3000*g* for 10 min, washed with phosphate-buffered saline (PBS) (10 mM, pH 7.4), and then resuspended in PBS to an optical density (OD_{600}) of 0.016. After that, the MIC of JCpep8 was incubated in the reaction tubes with 1 mL of media and 1 mL of the test microorganisms for different times at 37 °C under the same conditions. A total of 1 mL of PBS was used as the control. OD_{600} was read with a UV-2800 spectrophotometer (Unico, Shanghai, China).

Outer Membrane Disruption Assay. The experiment was investigated by means of the ANS uptake assay according to Thennarasu et al.[21] *S. aureus* of mid-log phase was centrifuged at 3000*g* for 10 min, and the precipitate was collected, washed by PBS (10 mM, pH 7.4) 10 times, then centrifuged again, and resuspended in PBS to an OD_{600} of 0.215. The MIC of JCpep8 was incubated in the reaction tubes with 0.2 mL of ANS (a final concentration of 5.65 mM) and 2.8 mL of the test microorganisms for different times at 37 °C. The extent of membrane disruption was observed by the changes of fluorescence intensity (F-7000 FL spectrophotometer, Shimadzu, Kyoto, Japan) at ∼450 nm.

Inner Membrane Disruption Assay. The experiment was performed according to Xiao et al.,[22] with some modifications. *S. aureus* of mid-log phase at 37 °C was centrifuged at 3000*g* for 10 min. Then, the precipitate was washed by PBS (10 mM, pH 7.4) 10 times and resuspended in PBS to an OD_{600} of 0.016. Subsequently, 1 mL of the test microorganisms and JCpep8 at the MIC was incubated in the reaction tubes for different times at 37 °C. The mixture was filtered with a 0.22 μm microporous membrane to remove the bacteria cells. Then, the OD_{600} of the filtrate at 260 nm was recorded. Strains incubated with PBS were used as the control.

Activity on the Bacterial Ultrastructure. *Fourier Transforms Infrared (FTIR) Spectroscopy.* The sample was prepared by the method described by Helm et al.,[23] with some modifications. *S. aureus* of mid-log phase was resuspended in deionized water to an OD_{600} of 0.124, and then the JCpep8 was added. Strains incubated with PBS (10 mM, pH 7.4) were used as the control. After incubation for 1.5 h at 37 °C, 50 μL suspensions of incubated strains and control were transferred to an transparent optical crystal (KBr). The suspensions were dried under vacuum using anhydrous silica gel (Shanghai, China) in a desiccator to form films, which were suitable for FTIR analysis (FTIR spectrometer, Thermo Electron Corporation). A total of 32 scans were collected for each sample at a resolution of 4 cm^{-1} in the range between 400 and 4000 cm^{-1}.

Transmission Electron Microscopy (TEM). The effect of JCpep8 on the ultrastructural morphology of *S. aureus* was assessed using TEM (Hitachi H-7000, Japan).[24] After treatment with JCpep8 for different times (0 and 1.5 h) at the MIC, the cells were immediately washed 3 times with PBS and fixed with 2.5% (v/v) glutaraldehyde.

Statistical Analysis. All experiments were performed in triplicates. The average value and standard deviation were calculated. The data were analyzed using SPSS 13.0 statistical software.

RESULTS AND DISCUSSION

Binding Constant. The initial binding to living bacteria has been considered as the most important physicochemical characteristic of AMPs. Recently, advances of CEC have been applied as an aid in the field of molecular biology for characterization of biomolecules by electrophoretic analysis of binding interactions. For example, EI-Hady et al. used CEC to characterize the interaction between drugs and proteins.[25] Berthod et al. probed the binding of vancomycin to *Bifidobacterium infantis* using CEC.[26] Carrozzino et al. used liposome capillary electrophoresis to simulate the interactions between drugs and biomembrane.[27] Nilsson et al. used the nanoparticle as a pseudo-stationary phase in CEC for protein analysis.[28] In our present research, we have studied the binding characterizations of the interaction of JCpep8 with the LSAC model system using high-sensitivity CEC.

The electropherograms of JCpep8 with the same running buffer containing increasing amounts of LSACs at the different temperatures (298, 303, and 309 K) were shown in Figure 1. The migration time of the neutral marker (acetone) almost remained the same, which indicated that the increasing concentrations of LSACs did not affect the retention behavior of acetone; namely, the binding of acetone to LSACs was extremely weak or non-existent. In contrast, with the augmentation of the LSAC concentration, the migration time of JCpep8 increased as well; meanwhile, the peak of JCpep8 trended to be shorter and wider, which was ascribed to the increasingly generated binding of JCpep8 to LSACs. In addition, with the further increasing of the amount of LSACs, the peak became abnormal and distorted with a concomitant appearance of peaks of free LSACs. At the maximum LSAC concentration in the running buffer, JCpep8 migrated after the

dx.doi.org/10.1021/jf2052509 | J. Agric. Food Chem. 2012, 60, 4535−4541

Table 2. Thermodynamic Parameters of the Interaction between JCpep8 and LSACs.

temperature (K)	K (M^{-1})[a]	r^2	ΔH (J/mol)	ΔS (J mol^{-1} K^{-1})	ΔG (kJ/mol)
298	$7.40 \pm 0.20 \times 10^{11}$				−14.86
303	$1.43 \pm 0.08 \times 10^{12}$	0.9905	0.7	50.1	−15.11
309	$2.60 \pm 0.08 \times 10^{12}$				−15.41

[a]Mean ± SD (n = 3).

neutral electroosmotic flow (EOF) marker (top trace of Figure 1), suggesting that there is a significant interaction between JCpep8 and LSACs, and more and more spikes occurred in the baseline, which was a result of increasing LSACs presented in the running buffer passing through the ultraviolet (UV) detector and producing light scattering, suggested that the absorption of JCpep8 was saturation. A similar phenomenon was also found in refs 26 and 29−31. Table 1 listed the experimental data from the Figure 1 experiments. The binding constant of JCpep8 to LSACs determined by this linear plot was 7.4×10^{11} M^{-1} at 298 K, 1.43×10^{12} M^{-1} at 303 K, and 2.6×10^{12} M^{-1} at 309 K. The results showed that the interaction between JCpep8 and LSACs was significant. In fact, the accessible surface area of *S. aureus* can be 1000-fold larger than the surface area of JCpep8. Therefore, *S. aureus* can be combined with a number of JCpep8 molecules. Consequently, the binding constant measured in our paper was the total value of the binding constant, which contained all of the binding capacities of the sum of the binding sites. Similar results were reported by Berthod et al.[26] and Xia et al.[32] The reproducibility of the results was confirmed by repeating the whole experiment at different temperatures, and all of the repeating measurements were performed in the same day with the same batch of bacteria.

Interaction Forces. Although some interaction forces, such as the hydrophobic effect, electrostatic force, van der Waals force, and hydrogen bonds, existed between AMPs and bacteria,[1] the varied AMPs may have different forces in the binding process, which is usually characterized by the thermodynamic parameters. The thermodynamic parameters were determined by the van't Hoff equation ($\ln K = -\Delta H/RT + \Delta S/R$, and $\Delta G = \Delta H - T\Delta S$). In the equations, the reason for the criterion of data selection is that the measured heat is the sum of all thermal effects of the association process. Therefore, to characterize the binding forces between JCpep8 and LSACs, the thermodynamic parameters, such as ΔH, ΔS and ΔG, should be analyzed. As shown in Table 2, ΔG was less than zero, which revealed that the interaction process was spontaneous. On the basis of the previous theories reported by Ross and Subramanian,[19] ΔH (0.7 J/mol, almost zero) and ΔS (50.1 J mol^{-1} K^{-1}) in our study suggested that the electrostatic force and hydrophobic effect may play major roles in the binding processes of JCpep8 to LSACs.

Growth Inhibition Curve Assay. From the results of the binding experiment, it can be known that the interaction between JCpep8 and LSACs was significant. It is well-known that it is the first and critical step of AMPs to bind to bacteria to exert their antimicrobial activity. With no doubt, the bacterial growth behavior is indispensably affected by the binding process. The growth curve is the most direct indicator used to detect the bacterial growth behavior. Figure 2 showed the growth inhibition curve of JCpep8 for *S. aureus*. Before 60 min, the OD_{600} (experimental and control groups) raised slowly. At 90 min, the OD_{600} of the experimental group was lower than that of the control group, indicating that JCpep8 began to play

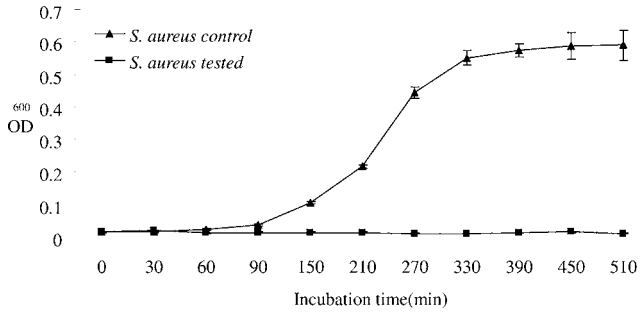

Figure 2. Growth inhibition curve of JCpep8. The concentration of JCpep8 was MIC (45 μg/mL) for *S. aureus*.

an effective role. At 150 min, the inhibition effect was obvious. Especially at 330 min, the OD_{600} of the experimental group vigorously increased, while the OD_{600} of the control group was kept stable, indicating that JCpep8 completely inhibited the division of *S. aureus*. The results suggested that the antibacterial effect of JCpep8 was quick, efficient, and time-dependent.

Outer Membrane Disruption Assay. From the results of the growth inhibition curve (Figure 2), bacterial growth was inhibited, indicating that bacterial cells have certainly been injured. Because the bacterial cell wall is the outermost layer of bacterial cells, whether the bacterial cell wall is injured or not is first checked. The abilities of JCpep8 to disrupt the bacterial membrane were investigated by monitoring the ANS uptake assay. A total of 0.2 mL of 5.65 mM ANS equilibrated with 2.8 mL of *S. aureus* cells showed a maximum emission at 477 nm (0 min in Figure 3). After successive treatment by JCpep8, the cell suspension resulted in an enhancement in the fluorescence intensity of ANS and a shift in the maximum emission. At 0 min, the observed maximum fluorescence intensity was 143.6 at 477 nm. In contrast, when treated for 210 min, a blue-shifted

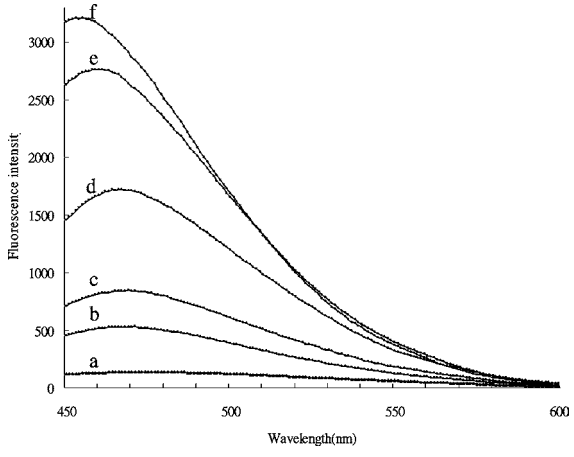

Figure 3. JCpep8-induced ANS binding to *S. aureus* at (a) 0 min, (b) 30 min, (c) 60 min, (d) 90 min, (e) 150 min, and (f) 210 min. The concentration of JCpep8 was MIC (45 μg/mL) for *S. aureus*.

maximum emission at 455 nm was found and the fluorescence intensity at this wavelength was 3206, which was 20 times higher than that at 0 min. It can be inferred that JCpep8 disrupted the outer membrane of *S. aureus*, which led ANS to relocate into a relatively hydrophobic environment.

Inner Membrane Disruption Assay. From Figures 2 and 3, it can be concluded that JCpep8 can completely inhibit the growth and disrupt the outer membrane of *S. aureus*. However, JCpep8-acted functions in detail are still unknown, and they are of considerable interest to understand. To explore whether the inner membrane may be broken apart, which leads to cell death when an effective concentration of JCpep8 bound to the inner membrane, the inner membrane permeability assay was performed. As seen from Figure 4, there was no UV absorption

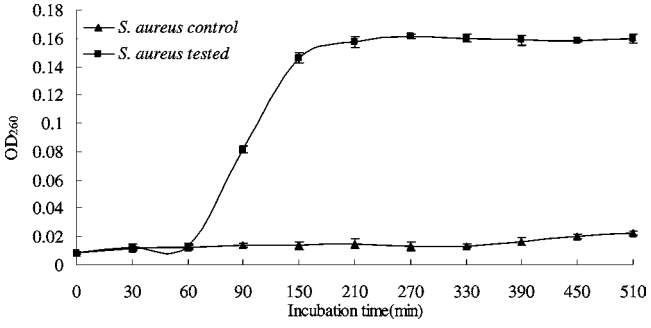

Figure 4. Total nucleotide leakage from *S. aureus* treated with JCpep8. The concentration of JCpep8 was MIC (45 μg/mL) for *S. aureus*.

(OD_{260}) after treatment by JCpep8 in the initial stage (0–60 min). However, starting from 60 min, the spilled UV absorption material was dependent upon the incubation time. With treatment by 90 min, the permeability rate was nearly 50%. With treatment by 210 min, the permeability rate was nearly 100%. Under normal circumstances, only the molecules, which are less than 1 nm, can pass through the micropores on the bacterial cell membrane.[17] The experimental results showed that, with the extended duration of JCpep8, the bacterial cell permeability barrier of the inner membrane was damaged, resulting in the leakage of intracellular UV absorption materials, while there was no leakage of UV absorption materials from the cells in the control group.

Activity on the Bacterial Ultrastructure. The above results showed that the bacteria died from the damage of cell walls and membranes caused by JCpep8. To further elucidate the nature of the killing mechanisms of JCpep8, *S. aureus* treated with JCpep8 for 0 min and 1.5 h was analyzed by FTIR and TEM. FTIR spectra (4000–400 cm^{-1}) can be applied in identifying microbial cells at the strain level and has been widely recognized.[33−35] FTIR spectra of microorganisms, which represents the total biochemical composition of the bacterial cell wall and membrane and cellular cytoplasm, are usually divided into five regions[36] to describe different cell component information: (1) 3000–2800 cm^{-1}, fatty acids in the bacterial cell membrane; (2) 1800–1500 cm^{-1}, amide bands from proteins and peptides; (3) 1500–1200 cm^{-1}, mixed region of proteins and fatty acids; (4) 1200–900 cm^{-1}, polysaccharides within the cell wall; and (5) 900–500 cm^{-1}, "true" fingerprint region containing bands. As shown in Figure 5, the differences were observed in the FTIR absorption spectra, mainly concerning the spectral shape of the band of proteins and fatty acids (1500–1200 cm^{-1}). Through the above analysis, it can be clearly seen that JCpep8 affected the structure of the *S. aureus* cell wall and membrane mainly by cutting off the connections of some of the groups (such as RNH_2, R_2NH, etc.)

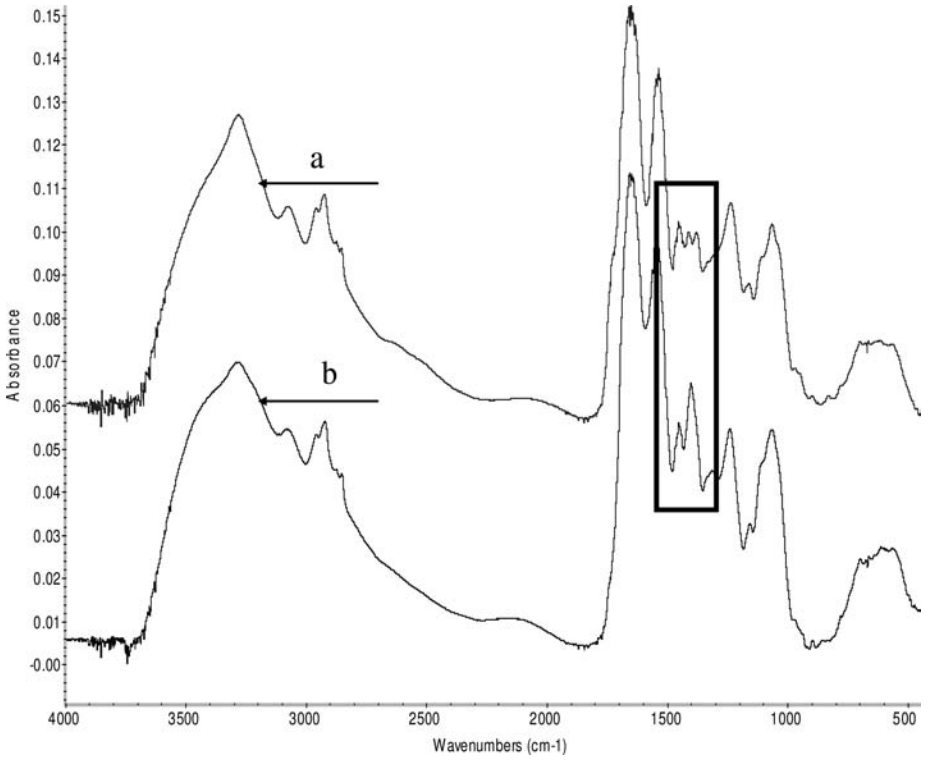

Figure 5. FTIR absorption spectrum of the *S. aureus* (a) cell after treatment with JCpep8 for 1.5 h and (b) control cell. The concentration of JCpep8 was MIC (45 μg/mL) for *S. aureus*.

to play a bactericidal effect. The results that AMPs can affect the structure of membrane composition have been reported in the literature as well.[37]

TEM was used to directly observe the damage of bacterial cells and changes in the cell ultrastructure. As shown in Figure 6, the surface of the control cell (Figure 6A) was smooth,

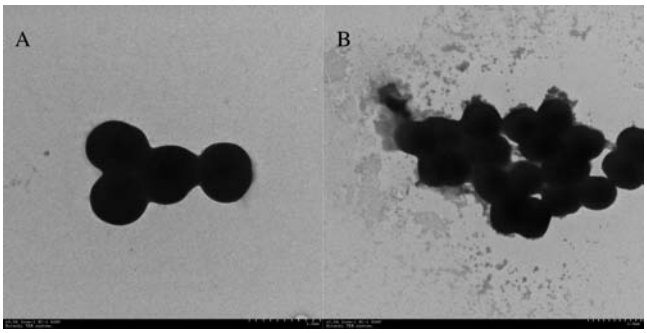

Figure 6. Morphological changes of *S. aureus* upon incubation with JCpep8 of the (A) control cell and (B) cell after treatment with JCpep8 for 1.5 h. The concentration of JCpep8 was MIC (45 μg/mL) for *S. aureus*.

maintained integrity, was clearly visible, and was not damaged. In comparison to the control, the treated cell (Figure 6B) had obvious morphological changes. After 1.5 h of treatment, the surface of the treated cell in the field of vision was blurred and rough, indicating that, the longer the treatment time, the greater the extravasations adsorbed on *S. aureus*. Some protoplasm leak and cytoplasmic dilution were observed after treatment. However, completely distorted and ruptured bacterial cells were not found.

The same phenomenon was reported by Hallock et al.[38] It is the premise of a complete breakdown of the membrane that AMPs bound and inserted into the cell membrane. AMPs can cause the changes of membrane curvature, so that the structure of the lipid bilayer membrane is unstable or causes changes in other properties, leading to cell death.

Assuming that the antimicrobial model of JCpep8 was a "carpet model", the *S. aureus* cells were broken and incomplete.[1] However, cell debris has not been observed. Therefore, it may be inferred that JCpep8 played a bactericidal effect as follows. First, JCpep8 can penetrate the cell wall and then aggregate on the cell membrane to form holes, resulting in the leak of intracellular UV absorption materials. These data correlated with the binding constant (Table 1), outer membrane disruption assay, and inner membrane disruption assay after peptide treatment (Figures 3 and 4).

From the present study, the details of antimicrobial functions of JCpep8 in the living cell environment of *S. aureus* can be expressed with the following steps: (i) Prior to the interaction with the cell membrane, the positive-charged JCpep8 can first and rapidly bind with the cell wall, because of electrostatic attraction and hydrophobic interactions. (ii) Once bound to the cell wall, JCpep8 can break the cell wall, then continue to move forward to reach the cell membrane, and gather. When the concentration of gathered JCpep8 was beyond a certain threshold, it was able to form stable membrane holes in the cell membrane and the multiporous suface was formed. Subsequently, because of the increase of membrane permeability, intracellular material of bacteria leaked and the bacteria died. It is worth mentioning that the results of FTIR and TEM also confirmed the antimicrobial mechanism of JCpep8.

In conclusion, the results derived from this experiment can be seen that, unlike conventional antibiotics, which generally inhibit the biosynthesis of macromolecules and may selectively induce resistance in microbes, JCpep8 killed microbes mainly by wall-/membrane-targeting pore-forming mechanisms, which was more difficult for microbes to develop resistance. Therefore, the discovered antimicrobial details of JCpep8 provide a theoretical basis and are beneficial for developing new AMPs.

AUTHOR INFORMATION

Corresponding Author

*Telephone: +86-139-211-77990. Fax: +86-510-853-29099. E-mail: zhanghui@jiangnan.edu.cn.

Funding

This work was financially supported by the Program for Postgraduates Research Innovation in University of Jiangsu Province (CXZZ11_0493) and the fund (JUDCF09023) provided by Jiangnan University.

Notes

The authors declare no competing financial interest.

REFERENCES

(1) Brogden, K. Antimicrobial peptides: Pore formers or metabolic inhibitors in bacteria? *Nat. Rev. Microbiol.* **2005**, *3*, 238−250.

(2) Hoskin, D. W.; Ramamoorthy, A. Studies on anticancer activities of antimicrobial peptides. *Biochim. Biophys. Acta, Biomembr.* **2008**, *1778*, 357−375.

(3) Marsh, E. N. G.; Buer, B. C.; Ramamoorthy, A. Fluorine—A new element in the design of membrane-active peptides. *Mol. BioSyst.* **2009**, *5*, 1143−1147.

(4) Bhattacharjya, S.; Ramamoorthy, A. Multifunctional host defense peptides: Functional and mechanistic insights from NMR structures of potent antimicrobial peptides. *FEBS J.* **2009**, *276*, 6465−6473.

(5) Ramamoorthy, A.; Lee, D.-K.; Narasimhaswamy, T.; Nanga, R. P. R. Cholesterol reduces pardaxin's dynamics—A barrel-stave mechanism of membrane disruption investigated by solid-state NMR. *Biochim. Biophys. Acta, Biomembr.* **2010**, *1798*, 223−227.

(6) Pokorny, A.; Almeida, P. F. F. Kinetics of dye efflux and lipid flip-flop induced by δ-lysin in phosphatidylcholine vesicles and the mechanism of graded release by amphipathic, α-helical peptides. *Biochemistry* **2004**, *43*, 8846−8857.

(7) Ehrenstein, G.; Lecar, H. Electrically gated ionic channels in lipid bilayers. *Q. Rev. Biophys.* **1977**, *10*, 1−34.

(8) Ludtke, S. J.; He, K.; Heller, W. T.; Harroun, T. A.; Yang, L.; Huang, H. W. Membrane pores induced by magainin. *Biochemistry* **1996**, *35*, 13723−13728.

(9) Matsuzaki, K.; Murase, O.; Fujii, N.; Miyajima, K. An antimicrobial peptide, magainin 2, induced rapid flip-flop of phospholipids coupled with pore formation and peptide translocation. *Biochemistry* **1996**, *35*, 11361−11368.

(10) Shai, Y. Mode of action of membrane active antimicrobial peptides. *Pept. Sci.* **2002**, *66*, 236−248.

(11) Thennarasu, S.; Lee, D.-K.; Poon, A.; Kawulka, K. E.; Vederas, J. C.; Ramamoorthy, A. Membrane permeabilization, orientation, and antimicrobial mechanism of subtilosin A. *Chem. Phys. Lipids* **2005**, *137*, 38−51.

(12) Ayyalusamy, R. Beyond NMR spectra of antimicrobial peptides: Dynamical images at atomic resolution and functional insights. *Solid State Nucl. Magn. Reson.* **2009**, *35*, 201−207.

(13) Yeaman, M. R.; Yount, N. Y. Mechanisms of antimicrobial peptide action and resistance. *Pharmacol. Rev.* **2003**, *55*, 27−55.

(14) Rzepiela, A. J.; Sengupta, D.; Goga, N.; Marrink, S. J. Membrane poration by antimicrobial peptides combining atomistic and coarse-grained descriptions. *Faraday Discuss.* **2009**, *144*, 431−443.
(15) Epand, R. M.; Vogel, H. J. Diversity of antimicrobial peptides and their mechanisms of action. *Biochim. Biophys. Acta, Biomembr.* **1999**, *1462*, 11−28.
(16) Szumski, M.; Klodzinska, E.; Buszewski, B. Separation of microorganisms using electromigration techniques. *J. Chromatogr., A* **2005**, *1084*, 186−193.
(17) Joklik, W.; Willett, H.; Amos, D.; Wilfert, C. Staphylococcus. In *Zinsser Microbiology*, 20th ed.; Joklik, W. K., Willet, H. P., Amos, D. B., Eds.; Appleton and Lange: East Norwalk, CT, 1992; pp 401−416.
(18) Tanaka, Y.; Terabe, S. Estimation of binding constants by capillary electrophoresis. *J. Chromatogr., B: Anal. Technol. Biomed. Life Sci.* **2002**, *768*, 81−92.
(19) Ross, P.; Subramanian, S. Thermodynamics of protein association reactions: Forces contributing to stability. *Biochemistry* **1981**, *20*, 3096−3102.
(20) Hultmark, D.; Steiner, H.; Rasmuson, T.; Boman, H. G. Insect immunity. Purification and properties of three inducible bactericidal proteins from hemolymph of immunized pupae of *Hyalophora cecropia*. *Eur. J. Biochem.* **1980**, *106*, 7−16.
(21) Thennarasu, S.; Tan, A.; Penumatchu, R.; Shelburne, C. E.; Heyl, D. L.; Ramamoorthy, A. Antimicrobial and membrane disrupting activities of a peptide derived from the human cathelicidin antimicrobial peptide LL37. *Biophys. J.* **2010**, *98*, 248−257.
(22) Xiao, J.; Zhang, H.; Niu, L.; Wang, X. Efficient screening of a novel antimicrobial peptide from *Jatropha curcas* by cell membrane affinity chromatography. *J. Agric. Food Chem.* **2011**, *59*, 1145−1151.
(23) Helm, D.; Labischinski, H.; Schallehn, G.; Naumann, D. Classification and identification of bacteria by Fourier transform infrared spectroscopy. *J. Gen. Microbiol.* **1991**, *137*, 69−79.
(24) Reimer, L.; Kohl, H. *Transmission Electron Microscopy: Physics of Image Formation*, 5th ed.; Springer Verlag: New York, 2008; Vol. *36*.
(25) El-Hady, D.; Kühne, S.; El-Maali, N.; Wätzig, H. Precision in affinity capillary electrophoresis for drug−protein binding studies. *J. Pharm. Biomed.* **2010**, *52*, 232−241.
(26) Berthod, A.; Rodriguez, M.; Armstrong, D. W. Evaluation of molecule−microbe interactions with capillary electrophoresis: Procedures, utility and restrictions. *Electrophoresis* **2002**, *23*, 847−857.
(27) Carrozzino, J. M.; Khaledi, M. G. Interaction of basic drugs with lipid bilayers using liposome electrokinetic chromatography. *Pharm. Res.* **2004**, *21*, 2327−2335.
(28) Nilsson, C.; Becker, K.; Harwigsson, I.; Bülow, L.; Birnbaum, S.; Nilsson, S. Hydrophobic interaction capillary electrochromatography of protein mutants. Use of lipid-based liquid crystalline nanoparticles as pseudostationary phase. *Anal. Chem.* **2008**, *81*, 315−321.
(29) Okun, V.; Ronacher, B.; Blaas, D.; Kenndler, E. Capillary electrophoresis with postcolumn infectivity assay for the analysis of different serotypes of human rhinovirus (common cold virus). *Anal. Chem.* **2000**, *72*, 2553−2558.
(30) Okun, V. M.; Moser, R.; Ronacher, B.; Kenndler, E.; Blaas, D. VLDL receptor fragments of different lengths bind to human rhinovirus HRV2 with different stoichiometry. *J. Biol. Chem.* **2001**, *276*, 1057−1062.
(31) Okun, V. M.; Ronacher, B.; Blaas, D.; Kenndler, E. Affinity capillary electrophoresis for the assessment of complex formation between viruses and monoclonal antibodies. *Anal. Chem.* **2000**, *72*, 4634−4639.
(32) Xia, Z. N.; Li, L. X.; Yang, J.; Xiong, C. Q. Investigation of interaction between the drug and cell membrane by capillary electrophoresis. *Sci. China, Ser. B: Chem.* **2009**, *52*, 2200−2204.
(33) Orsini, F.; Ami, D.; Villa, A.; Sala, G.; Bellotti, M.; Doglia, S. FTIR microspectroscopy for microbiological studies. *J. Microbiol. Methods* **2000**, *42*, 17−27.
(34) Helm, D.; Naumann, D. Identification of some bacterial cell components by FTIR spectroscopy. *FEMS Microbiol. Lett.* **1995**, *126*, 75−79.
(35) Fischer, G.; Braun, S.; Thissen, R.; Dott, W. FTIR spectroscopy as a tool for rapid identification and intra-species characterization of airborne filamentous fungi. *J. Microbiol. Methods* **2006**, *64*, 63−77.
(36) Naumann, D.; Helm, D.; Labischinski, H. Microbiological characterizations by FTIR spectroscopy. *Nature* **1991**, *351*, 81−82.
(37) Bhunia, A.; Ramamoorthy, A.; Bhattacharjya, S. Helical hairpin structure of a potent antimicrobial peptide MSI-594 in lipopolysaccharide micelles by NMR spectroscopy. *Chem.—Eur. J.* **2009**, *15*, 2036−2040.
(38) Hallock, K. J.; Lee, D. K.; Ramamoorthy, A. MSI-78, an analogue of the magainin antimicrobial peptides, disrupts lipid bilayer structure via positive curvature strain. *Biophys. J.* **2003**, *84*, 3052−3060.